Plane Wave Scattering and Absorption by Resistive-Strip and Dielectric-Strip Periodic Gratings

Tatiana L. Zinenko, Alexander I. Nosich, *Senior Member, IEEE,* and Yoichi Okuno, *Senior Member, IEEE*

***Abstract*—The problems of plane wave scattering by resistive and dielectric strip gratings are considered. The formulation involves a set of resistive-type boundary conditions that characterizes nonzero jumps in tangential field components. The method of solution is based on analytical inversion of the static part of the full-wave equations and results in a rapidly convergent numerical algorithm. The dependences of the transmitted, reflected, and absorbed power fractions on the electrical and material parameters are presented.**

***Index Terms*— Absorbing media, electromagnetic scattering, gratings, periodic structures, strip scatterers.**

I. Introduction

THERE has been continuous attention to the problem of wave scattering by a flat-strip grating with zero thickness. This is because it is one of the canonical problems that attracts theoreticians' interest and has a wide range of applications that include microwave beam polarizers and diplexers. In addition, a solution to this problem can serve as a reference in validating a numerical code for a more complicated problem.

In a great number of research work, the strip-grating problem has been analyzed under the assumption that the strips were made of a perfect electric conductor (PEC) [1]–[4]. In this direction accurate results were obtained by the methods based on the analytical inversion of the static part (i.e., regularization) [2], [4] of the full-wave integral equation (IE). This procedure converts the original first-kind IE into a Fredholm second-kind one with a smooth kernel and, thus, proves the existence of a solution and convergence of standard discretization schemes. The difference between [2] and [4] may be found in the choice of the expansion functions employed: entire-period exponents and Chebyshev polynomials, respectively.

The use of PEC boundary conditions, however, prevents us from studying the absorption, which is of considerable interest for many practical applications. An important example is the case of a partially transparent thin-strip grating made of metal or dielectic. It is known that such a strip can be simulated by a combination of resistive-type boundary conditions [5]–[8]. Thus, the scattering of a plane wave from a resistive-strip grating is a key problem in this area as emphasized in several papers published previously [9]–[13]. A close view, however, reveals that in the H-wave case, the results have been obtained with no convergence; in the E-wave case, the previously used algorithms have been less efficient for narrow-strip or narrow-slot gratings. In part this was because none of the published analyses was based on the regularization concept. In [14], an analytical-regularization-based algorithm for studying the problem of a circularly curved resistive strip has been developed; in [15] it has been extended to a nonuniformly resistive reflector. The goal of the present paper is to apply this approach to the problems of the resistive and dielectric strip gratings.

The paper is organized as follows. Section II deals with the scattering of H- and E-waves by a resistive strip grating. Here, the boundary conditions involve an electrical resistivity that characterizes a nonzero jump of the tangential magnetic field. Two polarization cases are handled separately to cope with the different features of the basic equations. Section III extends our approach to the problem of a thin dielectric grating. Here, the introduction of magnetic resistivity is required to characterize the jump in the tangential electric field that eventually involves the solution of both types of equations met in Section II. In Section IV, we derive uniform low-frequency asymptotics based on the analytical iterations. Section V summarizes the conclusions. In the paper, the time dependence is assumed as $e^{-i\omega t}$ and omitted.

II. Resistive Strip Grating

A. Formulation

Let us consider the scattering of an incident plane wave from a grating consisting of zero-thickness resistive strips. Fig. 1 shows the geometry of the problem: the grating is periodic in the y-direction with a period l and is uniform in the x direction. The strip width is w and, hence, the slot width is $d = l - w$. In the E-wave case we assume that an x-polarized plane wave $\vec{E}^{in}(y, z) = \vec{u}_x U^{in}(y, z)$ is incident; while in the H-wave case we take $\vec{H}^{in}(y, z) = \vec{u}_x U^{in}(y, z)$ as the incident wave. Here,

$$U^{in}(y, z) = e^{-ik_0 z \sin\beta - ik_0 y \cos\beta} \tag{1}$$

is a scalar plane wave illuminating the grating at an angle of incidence β. The function $U = U^{in} + U^{sc}$, which denotes the x component of the total magnetic or electric field depending on the polarization, must satisfy the two-dimensional (2-D) Helmholtz equation

$$(\nabla^2 + k_0^2)U(\vec{r}) = 0, \quad k_0 = \omega(\epsilon_0\mu_0)^{1/2}, \quad \vec{r} = (y, z) \tag{2}$$

Manuscript received July 8, 1997; revised January 12, 1998. The work of T. L. Zinenko was supported by the Ministry of Education, Science, Sports, and Culture of Japan (Monbusho) in the form of a post-graduate scholarship.

T. L. Zinenko and Y. Okuno are with the Department of Electrical and Computer Engineering, Kumamoto University, Kumamoto, 860-8555 Japan.

A. I. Nosich is with the Institute of Radiophysics and Electronics, National Academy of Sciences, Kharkov 310085, Ukraine.

Publisher Item Identifier S 0018-926X(98)07498-5.

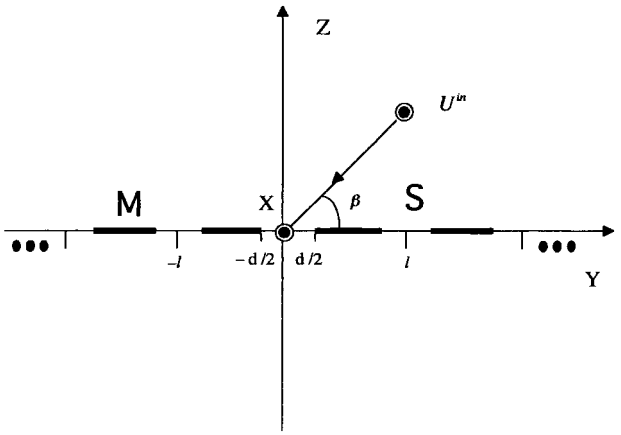

Fig. 1. Geometry of the strip grating scattering problem. M and S denote the strip and slot, respectively.

under the conditions C1)–C3) given below, which guarantee the uniqueness of solution.

C1) The set of resistive-surface boundary conditions [7] couples the tangential field components on the strip surface M: $\{z = 0,\ |y - l/2 - ml| < w/2,\ m = 0, \pm 1, \cdots\}$

$$\tfrac{1}{2}[\vec{E}_T^+(\vec{r}) + \vec{E}_T^-(\vec{r})] = Z_0 R \vec{n} \times [\vec{H}_T^+(\vec{r}) - \vec{H}_T^-(\vec{r})], \tag{3}$$

$$\vec{E}_T^+(\vec{r}) = \vec{E}_T^-(\vec{r}). \tag{4}$$

The plus (or minus) superscript means that the quantity is the limiting value from the upper (lower) side of the strip M. Here, $\vec{n} = \vec{z}_0$, Z_0 is the free-space impedance, and R is the normalized electric resistivity simulating either a thin dielectric layer or a thinner-than-skin-depth layer of imperfect metal. Respective formulas for R are [5], [8]

$$R_{\text{diel}} = i[k_0 h(\epsilon_r - 1)]^{-1}, \qquad R_{\text{met}} = (Z_0 h \sigma)^{-1} \tag{5}$$

where h is the strip thickness, ϵ_r is the relative permittivity, and σ is the conductivity.

C2) Strictly speaking, (3) and (4) do not hold at the strip edges. There, the field should meet the condition of finite stored energy

$$\int_D (\epsilon_0 |\vec{E}|^2 + \mu_0 |\vec{H}|^2)\, dy\, dz < \infty \tag{6}$$

where D is an arbitrary finite domain enclosing an edge point.

C3) The radiation condition eliminates, in the scattered field U^{sc}, any waves that do not comply with the principle "*no sources at infinity*," i.e., in our case, at $z \to \pm\infty$.

Besides these conditions, the Poynting theorem results in the power conservation law

$$1 = P_{\text{ref}} + P_{\text{tr}} + P_{\text{abs}} \tag{7}$$

where P_{ref}, P_{tr}, and P_{abs} are the power fractions reflected, transmitted, and absorbed by the grating, respectively ($P_{\text{abs}} = 0$ in the lossless case of $\operatorname{Re} R = 0$). They relate to a single period of the grating and are normalized to the power carried, at one period, by the incident wave.

B. Solution Methods

The total strip domain M is an infinite-periodic set of the zero-thickness strips along the y axis and the incident field $U^{in}(y, z)$ is a pseudoperiodic function of y as suggested by (1). Hence, the scattered field $U^{sc}(y, z)$ is also a pseudoperiodic function of y and, thus, can be expanded in terms of a Floquet–Rayleigh series such as

$$U^{sc}(y, z) = \sum_{n=-\infty}^{\infty} \begin{Bmatrix} a_n, & z > 0 \\ b_n, & z < 0 \end{Bmatrix} \times e^{ik_0 g_n |z|} e^{i((2\pi n/l) - k_0 \cos\beta) y} \tag{8}$$

Here, a_n and b_n are the Floquet-mode amplitudes (complex numbers) of the scattered field in the reflection and transmission half-space, respectively. Besides, $g_n = [1 - (n/\kappa - \cos\beta)^2]^{1/2}$ and $\kappa = k_0 l/2\pi = l/\lambda$, λ being the wavelength. Note that the radiation condition requires that for each mode, either $\operatorname{Re} g_n > 0$, or $\operatorname{Im} g_n > 0$. Expansions in (8) lead us to the following expressions for the normalized power fractions involved in (7):

$$P_{\text{ref}} = g_0^{-1} \sum_{|n - \kappa\cos\beta| < \kappa} g_n |a_n|^2,$$
$$P_{\text{tr}} = g_0^{-1} \sum_{|n - \kappa\cos\beta| < \kappa} g_n |b_n + \delta_{0n}|^2 \tag{9}$$

where δ_{0n} is the Kronecker delta, and summation is taken over the modes that carry power to infinity.

Let us consider first the H-wave case, where $\vec{H}_T = H_x \vec{x}_0$, $\vec{E}_T = E_y \vec{y}_0$, and $E_y = -(Z_0/ik_0)\partial H_x/\partial z$. The amplitudes of the modes a_n and b_n are coupled by the boundary conditions (3) and (4) on M and the continuity conditions across the slot domain S. Hence, the equation $E_y^+ = E_y^-$ is valid for all y and $z = 0$. This yields $b_n = -a_n$, so one set of coefficients, say, b_n can be excluded from further consideration.

To determine the coefficients a_n, let us use a dual set of boundary conditions that hold on the complementary subintervals M and S on the y axis, namely

$$\tfrac{1}{2}(E_y^+ + E_y^-) = Z_0 R (H_x^+ - H_x^-), \qquad (y, z) \in M \tag{10}$$

$$H_x^+ = H_x^-, \qquad (y, z) \in S. \tag{11}$$

By introducing the notations $\phi = 2\pi y/l$, $\theta = \pi d/l$, and

$$r_n = |n| + i[\kappa^2 - (n - \kappa\cos\beta)^2]^{1/2} = |n| + i\kappa g_n \tag{12}$$

and using the series expansion (8), we arrive at the dual series equations (DSE)

$$\begin{cases} \displaystyle\sum_{n=-\infty}^{\infty} a_n |n| e^{in\phi} = -i\kappa \sin\beta \\ \qquad \displaystyle + \sum_{n=-\infty}^{\infty} a_n (r_n + i2\kappa R) e^{in\phi}, & \theta < |\phi| \le \pi \\ \displaystyle\sum_{n=-\infty}^{\infty} a_n e^{in\phi} = 0, & |\phi| < \theta. \end{cases} \tag{13}$$

These DSE are of canonical form, whose left-hand side forms the Riemann–Hilbert problem (RHP) [2], [16], [17].

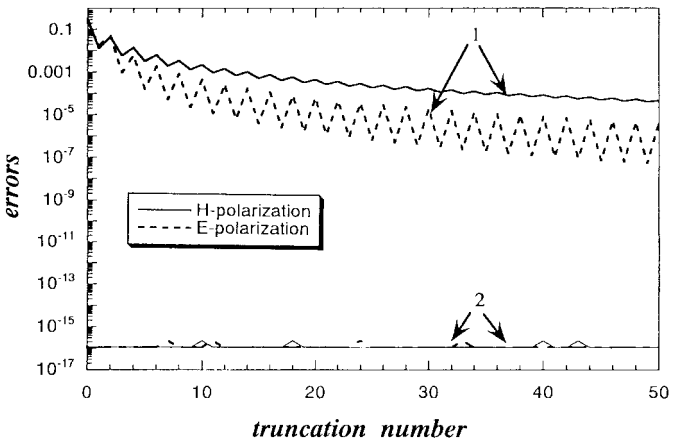

Fig. 2. (a) Normalized computation errors and (b) power conservation balance as a function of the matrix truncation number for the H-wave (solid curves) and E-wave (dashed curves). $\kappa = 1.5$, $\beta = 90^\circ$, $R = i$.

Exact analytical solution to the RHP, as given in [17], yields an infinite-matrix equation equivalent to (13)

$$a_m = \sum_{n=-\infty}^{\infty} a_n(r_n + i2\kappa R)T_{mn}(\theta) - i\kappa \sin\beta T_{m0}(\theta), \quad m = 0, \pm 1, \pm 2, \cdots \tag{14}$$

where the functions $T_{mn}(\theta)$ are given in the Appendix. Based on the large-index asymptotics of the Legendre polynomials, one can verify that $T_{mn} = O([|mn|^{-1/2}|m - n + 1|^{-1})$ uniformly for all θ. This is enough to prove that the operator norm $\|A\|^2 = \sum_{m,n=-\infty}^{\infty} |A_{mn}^H|^2 < \infty$ [here A_{mn}^H denotes the matrix elements of (14)] and, hence, (14) is a regularized matrix equation, i.e., of the Fredholm second kind. It can also be shown (see [17]) that the solution based on (14) satisfies the condition (6). This is due to the fact that the edge behavior is taken into account when inverting the RHP [2], [16], [17]. Note that if $\kappa = 0$ all the matrix elements are identically zero. This shows that (14) delivers an exact analytical solution in this limit.

Consider now the E-wave case. Then $\vec{E}_T = E_x\vec{x}_0$ and $\vec{H}_T = H_y\vec{y}_0$, with $H_y = (1/ik_0Z_0)\partial E_x/\partial z$. Instead of (10) and (11), we have now the dual conditions

$$\tfrac{1}{2}(E_x^+ + E_x^-) = -Z_0R(H_y^+ - H_y^-), \quad (y, z) \in M \tag{15}$$

$$H_y^+ = H_y^-, \quad (y, z) \in S. \tag{16}$$

By using these boundary conditions and the fact that $a_n = b_n$ holds in this polarization, we obtain a series equation as follows:

$$\sum_{n=-\infty}^{\infty} a_n g_n e^{in\phi} = \begin{cases} -\dfrac{1}{2R}\left(1 + \displaystyle\sum_{n=-\infty}^{\infty} a_n e^{in\phi}\right), & \theta < |\phi| \le \pi \\ 0, & |\phi| < \theta. \end{cases} \tag{17}$$

The left-hand side of (17) can be inverted analytically by using the inverse Fourier transformation and the orthogonality of the exponents. This leads us to the following set of equations:

$$a_m = -\frac{1}{2Rg_m}\sum_{n=-\infty}^{\infty} a_n S_{mn}(\theta) - \frac{1}{2Rg_m} S_{m0}(\theta), \quad m = 0, \pm 1, \pm 2, \cdots \tag{18}$$

where the functions $S_{mn}(\theta)$ are given in the Appendix. For any $R \neq 0$, this is a regularized infinite-matrix equation since $\sum_{m,n=-\infty}^{\infty} |A_{mn}^E|^2 < \infty$, A_{mn}^E being the matrix elements. Further, note that the rate of decay of the matrix elements of (18) with respect to the large $|m|$ and large $|n|$ is different. To symmetrize it, we introduce new variables $x_n = a_n w_n$ with the weight $w_n = (|n| + 1)^{1/2}$ and we arrive at

$$x_m = -\frac{w_m}{2Rg_m}\sum_{n=-\infty}^{\infty} x_n \frac{1}{w_n} S_{mn}(\theta) - \frac{w_m}{2Rg_m} S_{m0}(\theta). \tag{19}$$

Solving this matrix equation has a preference over (18), for the same accuracy, due to a more rapid decrement of the elements. Note also that if $\kappa = 0$, matrix elements of both (18) and (19) vanish identically; this means that the static problem is solved analytically.

C. Numerical Results

The matrix equations (14) and (19) can be used to compute the coefficients a_n and b_n whatever the parameters κ, β, and d/l are. The regularized nature of these equations guarantees that the greater the number of equations $N_{\rm tr}$, the smaller the error in the approximate numerical solution. Thus, the accuracy is limited only by the digital precision of the computer used. In fact, the truncation number needed for, say, a uniform three-digit accuracy, does not depend on d/l and β; it is found empirically that in the H-wave case $N_{tr} = \kappa(1 + |R|^{1/2}) + 10$. Our computations have shown an agreement within one to three digits with the previously published data [9]–[13]. However, here a correct conclusion should be done. Comparing the matrix equation (14) with its H-wave counterparts in [9], [11], and [12], one may easily see that the latter have the elements that do not decrease with large m and, hence, unable to yield a convergent solution for a progressively larger $N_{\rm tr}$. Our algorithm, on the contrary, shows a rapid decrement of the relative truncation error as demonstrated in Fig. 2 (see [14] for the definition of the relative truncation error). The matrix equation (19) is somewhat similar to its E-wave counterparts in [9], [10], and [12] due to the fact that the resistive boundary condition leads us immediately to a Fredholm second-kind IE for the current; hence, no analytical regularization is needed. The unknown current density function here has no singularity at the edges of a resistive strip. Computationally, any reasonable discretization scheme yields a regularized matrix equation. Our choice of entire-period exponents as expansion functions has a merit that the algorithm efficiency does not depend on the d/l value. A uniform three-digit accuracy in the E-wave case is achieved with $N_{tr} = \kappa(1+|R|^{-1/2})+10$. The truncation error

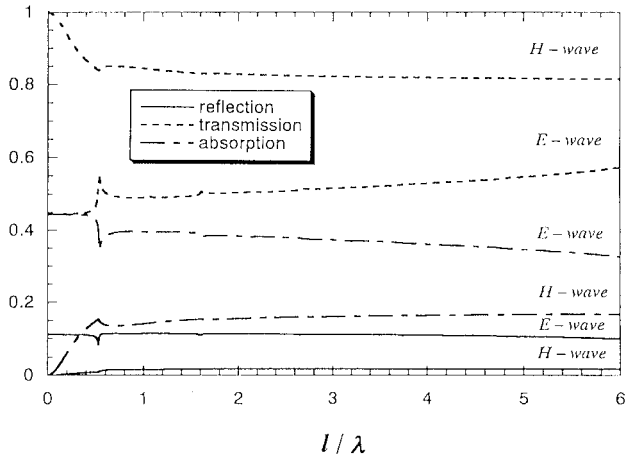

Fig. 3. Transmitted, reflected, and absorbed power fractions for the scattering by a resistive-strip grating versus the electrical period. $\beta = 30^\circ$, $d/l = 0.5$, $R = 1$.

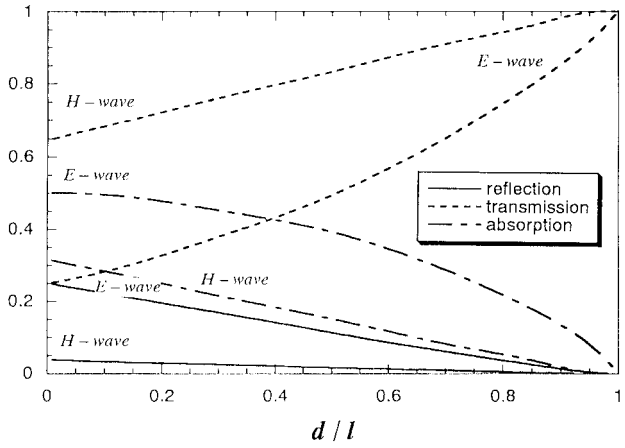

Fig. 4. Power fractions for the scattering by a resistive-strip grating versus the relative slot width. $\beta = 30^\circ$, $\kappa = 1.5$, $R = 1$.

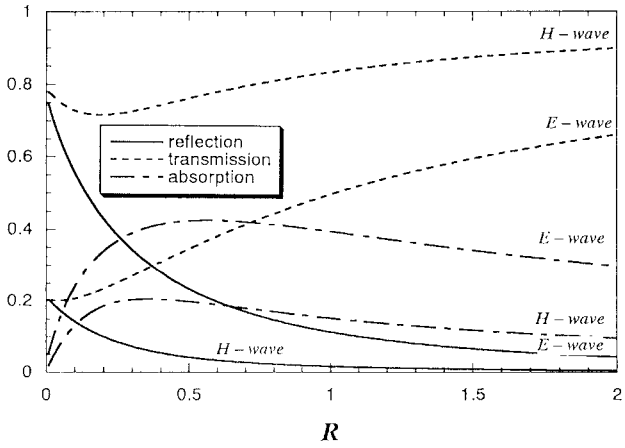

Fig. 5. Power fractions for the scattering by a resistive-strip grating versus the normalized strip resistivity value. $\beta = 30^\circ$, $\kappa = 1.5$, $d/l = 0.5$.

here decays with oscillations (Fig. 2). Note that the power conservation law is always satisfied to the machine precision, even if the number of equations is small. Hence, an agreement with [9]–[13] should be interpreted as a partial validation of the latter results if obtained by nonconvergent techniques.

In Fig. 3, we present the values of the transmitted, reflected and absorbed power fractions as a function of the electrical period of the grating (i.e., the period normalized by the wavelength). They show that for realistic values of electric resistivity, the power absorbed is quite comparable with the scattered power. The Wood anomalies are observed when a harmonic is "passing over horizon," in the form of abrupt extrema (the curve derivative has singularities of the square-root-type at these points). However, they are less strong than in the PEC case. The analysis of the power dependences on the relative width of the slot (Fig. 4) shows the decrement of the scattered and absorbed power fractions with the strip width. We emphasize here that our algorithm is equally efficient for arbitrary strip/slot ratio of the grating. Interestingly, the absorption power as a function of the normalized real-valued electric resistivity (Fig. 5) demonstrates existence of a broad maximum of which amplitude and position depend on the relative width of the strip and the angle of incidence. This is because the initial growth of absorption, with increasing R, is further cancelled by an increased transmission. The reflected power undergoes a larger degradation than the transmitted one; this fact has been reported previously for a different resistive periodic surface [18].

III. Dielectric Strip Grating

A. Formulation

Consider now a plane wave incident on a thin dielectric strip grating. We assume that the geometry is the same as before (Fig. 1) and the strips have zero thickness; however, the following modified set of boundary conditions at the surface of the strips M is introduced [7]

$$\tfrac{1}{2}\left[\vec{E}_T^{+}(\vec{r}) + \vec{E}_T^{-}\right] = Z_0 R \vec{n} \times \left[\vec{H}_T^{+}(\vec{r}) - \vec{H}_T^{-}(\vec{r})\right] \qquad (20)$$

$$\frac{1}{2}\left[\vec{H}_T^{+}(\vec{r}) + \vec{H}_T^{-}(\vec{r})\right] = -\frac{1}{Z_0} Q \vec{n} \times \left[\vec{E}_T^{+}(\vec{r}) - \vec{E}_T^{-}(\vec{r})\right] \qquad (21)$$

where R and Q are the normalized electric and magnetic resistivities simulating a thin material layer. Following [7], we set

$$R = \frac{i}{2} Z \cot\left[\frac{1}{2}(\epsilon_r \mu_r)^{1/2} k_0 h\right]$$
$$Q = \frac{i}{2Z} \cot\left[\frac{1}{2}(\epsilon_r \mu_r)^{1/2} k_0 h\right]$$
$$Z = \left(\frac{\mu_r}{\epsilon_r}\right)^{1/2}. \qquad (22)$$

The edge condition and the radiation condition are the same as in the previous section. Here, of course, (6) leads to a different edge behavior from the resistive-strip problem. For a detailed discussion on this question see [19]. Note also that the formulas (22) permit a transition to the PEC case (that is, $R = i0$ and $Q = i\infty$) by fixing the product $\epsilon_r \mu_r$ and letting $|\epsilon_r| \to \infty$. Generally, (22) is valid for the high-contrast case, i.e., the case where the following inequalities hold simultaneously [7]: $k_0 h \ll 1$ and $|\epsilon_r \mu_r| \gg 1$.

In the case of low contrast, i.e., if the second of the above is not true, one should use, instead of (22), the first option of (5) and a similar formula for the magnetic resistivity [7],

[8]: $Q = i[k_0 h(\mu_r - 1)]^{-1}$. Nevertheless, conditions (20) and (21) with the resistivities (22) have an important feature: they describe the case of the full transparency ($R = Q = i0$) provided that $(\epsilon_r \mu_r)^{1/2} k_0 h = (2n+1)\pi$, $n = 0, 1, 2, \cdots$. Of course, an accurate evaluation of the range of parameter variation ensuring a good accuracy of approximate conditions (20)–(22) needs a comparison with a solution of the original problem formulated without any approximation.

B. Solution Method

In the H-wave case we expand the scattered field as in (8). To determine the coefficients a_n and b_n, we use two scalar sets of dual conditions that come from (20) and (21); and we request that the total field is continuous across the slot:

$$\tfrac{1}{2}(E_y^+ + E_y^-) = Z_0 R(H_x^+ - H_x^-), \qquad (y, z) \in M;$$
$$H_x^+ = H_x^-, \qquad (y, z) \in S, \tag{23}$$
$$\frac{1}{2}(H_x^+ + H_x^-) = \frac{1}{Z_0} Q(E_y^+ - E_y^-), \qquad (y, z) \in M;$$
$$E_y^+ = E_y^-, \qquad (y, z) \in S. \tag{24}$$

By introducing the same notations as before we arrive at the two sets of the DSE as

$$\begin{cases} \displaystyle\sum_{n=-\infty}^{\infty} (a_n - b_n)|n| e^{in\phi} = -i2\kappa \sin\beta \\ \qquad + \displaystyle\sum_{n=-\infty}^{\infty} (a_n - b_n)(r_n + 2i\kappa R) e^{in\phi}, \quad \theta < |\phi| \le \pi \\ \displaystyle\sum_{n=-\infty}^{\infty} (a_n - b_n) e^{in\phi} = 0, \qquad |\phi| < \theta \end{cases} \tag{25}$$

$$\begin{cases} \displaystyle\sum_{n=-\infty}^{\infty} (a_n + b_n) g_n e^{in\phi} = -\frac{1}{Q} \\ \qquad -\displaystyle\frac{1}{2Q} \sum_{n=-\infty}^{\infty} (a_n + b_n) e^{in\phi}, \quad \theta < |\phi| \le \pi \\ \displaystyle\sum_{n=-\infty}^{\infty} (a_n + b_n) g_n e^{in\phi} = 0, \qquad |\phi| < \theta. \end{cases} \tag{26}$$

These DSE are of the form studied in the previous section. The left-hand side of each can be inverted analytically that yields equivalent decoupled infinite-matrix equations as

$$d_m = \sum_{n=-\infty}^{\infty} d_n (r_n + i2\kappa R) T_{mn}(\theta) - i2\kappa \sin\beta T_{m0}(\theta),$$
$$m = 0, \pm 1, \pm 2, \cdots \tag{27}$$
$$c_m = -\frac{w_m}{2Qg_m} \sum_{n=-\infty}^{\infty} c_n \frac{1}{w_n} S_{mn}(\theta) - \frac{w_m}{Qg_m} S_{m0}(\theta),$$
$$m = 0, \pm 1, 2, \cdots \tag{28}$$

where

$$d_n = a_n - b_n, \quad c_n = (a_n + b_n) w_n \tag{29}$$

and (28) has been symmetrized in the same way as it was done for (18).

Similarly in the E-wave case, we use the sets of dual boundary conditions as

$$\tfrac{1}{2}(E_x^+ + E_x^-) = -Z_0 R(H_y^+ - H_y^-), \qquad (y, z) \in M;$$
$$H_y^+ = H_y^-, \ (y, z) \in S \tag{30}$$
$$\frac{1}{2}(H_y^+ + H_y^-) = -\frac{1}{Z_0} Q(E_x^+ - E_x^-), \qquad (y, z) \in M;$$
$$E_x^+ = E_x^-, \ (y, z) \in S. \tag{31}$$

Then we obtain a pair of DSE's similar to (25) and (26). Further, we regularize them retracing all the steps in the H-wave case and come to the following pair of decoupled equations:

$$d_m = \sum_{n=-\infty}^{\infty} d_n (r_n + i2\kappa Q) T_{mn}(\theta) - i2\kappa \sin\beta T_{m0}(\theta),$$
$$m = 0, \pm 1, \pm 2, \cdots \tag{32}$$
$$c_m = -\frac{w_m}{2Rg_m} \sum_{n=-\infty}^{\infty} c_n \frac{1}{w_n} S_{mn}(\theta) - \frac{w_m}{Rg_m} S_{m0}(\theta),$$
$$m = 0, \pm 1, \pm 2, \cdots \tag{33}$$

where the definitions of c_n and d_n are the same as in (29).

C. Numerical Results

Figs. 6 and 7 demonstrate the values of the transmitted, reflected, and absorbed power fractions as a function of the electrical period of the grating with $\epsilon_r = 10 + i$ that roughly corresponds to wood permittivity. These values are given by (9) and coupled by the same power conservation law (7) as in the case of a resistive grating. Note that unlike in the previous section, here the resistivities R and Q are the functions of the frequency, thickness, and material parameters, and the solved matrix size must be adapted to their values. A characteristic feature of the plots in Figs. 6 and 7 is that they have a generally similar character for both polarizations that is different from the PEC or constant-resistivity case. Note that in the low-frequency limit, the strip grating is well transparent for an arbitrarily polarized plane wave and more power is absorbed than reflected. For a comparison, in the same figures the powers computed by using $R = R_{\text{diel}}$ of (5) and $Q = \infty$ are presented by the dotted curves. One may see that the low-contrast and high-contrast models agree well only in the low-frequency range. In the H-wave case the curves are monotonic, except for the small ripples in the Wood anomalies, but in the E-wave case a number of stronger resonances are observed. They belong to several different types according to the nature of a resonance. The most remarkable one is the narrow and deep drop of transmission near the $\pm$ first Wood's anomaly ($\kappa = 1$, for the normal incidence). Zooming this area shows that here both reflection and absorption have sharp maxima, the latter exceeding the former (see Fig. 8). So, a thin "wooden" grating of flat strips can serve as a narrow-band isolating screen. Comparison of these results with the similar ones (marked with triangles) computed by the volume integral equation (VIE) method of [20] shows a remarkably good agreement. This is due to the fact that in our approach, the approximation comes only in the model via introducing the

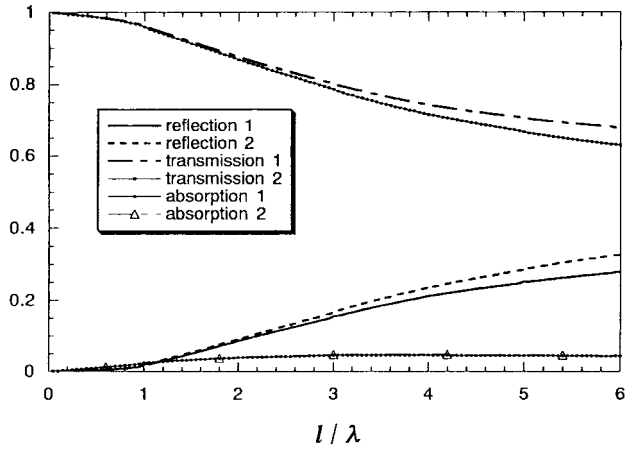

Fig. 6. Transmitted, reflected, and absorbed power fractions for the H-wave scattering by a dielectric strip grating versus the electrical period. $\beta = 90°$, $d/l = 0.5$, $h/l = 0.01$, $\epsilon_r = 10 + i$. Two models are compared: (a) high-contrast, i.e., R and Q based on (22) with $\mu_r = 1$ and (b) low-contrast, i.e., R based on the first of (5) and $Q = \infty$.

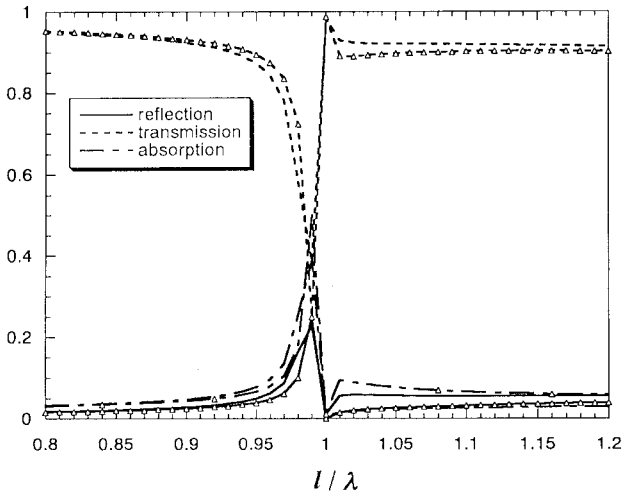

Fig. 8. The same as the high-contrast data in Fig. 7 but in the vicinity of the first Wood's anomaly. For comparison, similar data computed with the volume IE technique of [20] are presented by the marked curves.

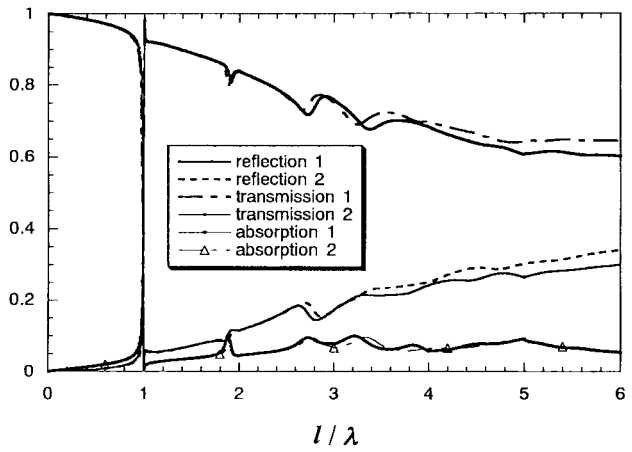

Fig. 7. The same as in Fig. 6 but for the E-wave.

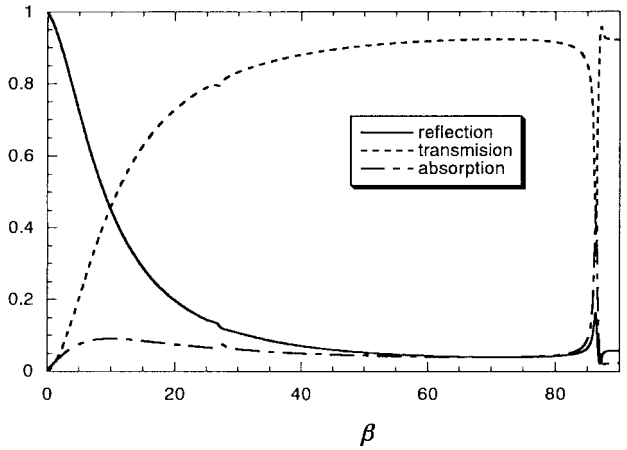

Fig. 9. Power fractions for the E-wave scattering by a dielectric strip grating versus the angle of incidence: $\kappa = 1.05$, $d/l = 0.5$, $h/l = 0.01$, $\epsilon_r = 10+i$, and $\mu_r = 1$.

resistivities R and Q, but not from the algorithm itself. This model is known as very accurate in the E-polarization case due to the absence of nontangential electric field. The results of VIE method can be considered as exact ones because in the case of E-polarization the VIE is of the Fredholm second kind, so the convergence of numerical solution is guaranteed. Central processing unit (CPU) expenditures of VIE method are naturally greater than in our treatment. In Fig. 9, we show the power fractions at $\kappa = 1.05$ versus the angle of incidence β for a dielectric-strip grating of the relative thickness $h/l = 0.01$ and $\epsilon_r = 10+i$. One may see that the effect of screening the E-polarized plane wave is observed in a narrow sector of angles.

IV. Modified Lamb's Formulas

Besides the guaranteed accuracy of numerical solution, the regularized matrix equations offer a way to derive analytical solutions by iterations. This important property is characteristic only to the Fredholm second-kind equations and is justified provided that the norm of the corresponding matrix operator $||A|| < 1$. As we have inverted the static parts of the full-wave equations, it is not surprising to see that in the each polarization case $||A|| < \kappa$ const. This means that in the low-frequency range the approximate formulas can be obtained after expanding all the quantities in terms of the power series of κ. Resulting low-frequency asymptotics will be uniform with respect to β and d/l. In doing this, we start from the constant-resistivity case of Section II and come to the following formulas for the H- and E-cases, respectively:

$$a_0^H = -b_0^H = \frac{-2i\kappa \sin\beta T_{00}(\theta) + O(\kappa^2)}{1 - i\kappa(\sin\beta + 2R)T_{00}(\theta)}$$
$$a_0^E = b_0^E = -\frac{S_{00}(\theta) + i\kappa(2\pi^2 R)^{-1}\alpha(\theta) + O(\kappa^2)}{2R\sin\beta + S_{00}(\theta)} \quad (34)$$

where $\alpha(\theta) = \sum_{n=1}^{\infty} \sin^2(n\theta) n^{-3}$. These formulas serve as modifications of the Lamb formulas [1], but unlike the latter they are obtained in a mathematically rigorous manner.

In the same way the matrix equations (27) and (28) and (32) and (33) yield the Lamb-type formulas for a dielectric strip due to a high contrast. Then, with the same accuracy as

in the previous case

$$\begin{pmatrix} a_0^H \\ b_0^H \end{pmatrix} = \mp \frac{i\kappa \sin\beta T_{00}(\theta)}{1 - i\kappa(\sin\beta + 2R)T_{00}(\theta)} - \frac{S_{00}(\theta) + i\kappa(2\pi^2 Q)^{-1}\alpha(\theta)}{2Q\sin\beta + S_{00}(\theta)} \tag{35}$$

$$\begin{pmatrix} a_0^E \\ b_0^E \end{pmatrix} = \mp \frac{i\kappa \sin\beta T_{00}(\theta)}{1 - i\kappa(\sin\beta + 2Q)T_{00}(\theta)} - \frac{S_{00}(\theta) + i\kappa(2\pi^2 R)^{-1}\alpha(\theta)}{2R\sin\beta + S_{00}(\theta)}. \tag{36}$$

If the frequency is even lower so that $\frac{1}{2}kh(\epsilon_r\mu_r)^{1/2} = \pi\kappa(h/l)(\epsilon_r\mu_r)^{1/2} \ll 1$ as well, a further simplification brings us to the following result:

$$\begin{pmatrix} a_0^H \\ b_0^H \end{pmatrix} = -i\kappa\left[\frac{\pm\sin\beta T_{00}(\theta)}{1 + 2(\epsilon_r h/l)^{-1}T_{00}(\theta)} + \frac{\mu_r(h/l)S_{00}(\theta)}{2\sin\beta + i\kappa\mu_r(h/l)S_{00}(\theta)}\right] \tag{37}$$

$$\begin{pmatrix} a_0^E \\ b_0^E \end{pmatrix} = -i\kappa\left[\frac{\pm\sin\beta T_{00}(\theta)}{1 + 2(\mu_r h/l)^{-1}T_{00}(\theta)} + \frac{\epsilon_r(h/l)S_{00}(\theta)}{2\sin\beta + i\kappa\epsilon_r(h/l)S_{00}(\theta)}\right]. \tag{38}$$

It is seen from (37) and (38) that a small-period dielectric strip grating is equally well transparent for an arbitrarily polarized plane wave, except for the case of grazing incidence ($\beta \approx 0$) that causes total reflection. The sector of near-grazing angles of good reflection is narrower for a smaller period of the grating. These considerations appear to be in agreement with the numerical results presented in Figs. 6, 7, and 9. The Lamb-type formulas can further be used for deriving the equivalent boundary conditions for a strip grating as uniform interface (so-called homogenization analysis) provided that the period is considerably smaller than the free-space wavelength.

V. Conclusions

We have presented a simple but numerically exact algorithm for computing the transmission, reflection, and absorption characteristics of an E- or H-polarized plane wave incident on a resistive or dielectric flat-strip periodic grating. Unlike the previously published solutions to these problems, here the accuracy is limited not by the method, but only by the digital precision of the computer used. Practically important is the fact that for a fairly good relative accuracy of 2–3 decimal places, one should take a rather small number of equations determined only by the relative period and resistivities but independent of the strip width and the angle of incidence. Besides, uniform low-frequency asymptotics have been derived for the scattering amplitudes in a mathematically rigorous manner.

Among the new features revealed by this accurate analysis is the existence of an optimum real-valued electric resistivity delivering a maximum absorption by a constant-resistivity strip grating, a similarity of low-frequency behavior of the E- and H-wave curves for a dielectric strip grating, and a quasi-total screening of the E-wave by a thin dielectric-strip grating near the first Wood's anomaly. In the case of a resistive grating, the results presented here coincide within a desired number of digits with similar data obtained by another regularization-type analysis: the singular-equation method of [4] modified for resistive strips in [21].

Appendix

1) Consider a DSE of the following form:

$$\begin{cases} \sum_{n=-\infty}^{\infty} x_n|n|e^{in\phi} = \sum_{n=-\infty}^{\infty} f_n e^{in\phi}, & \theta < |\phi| \le \pi \\ \sum_{n=-\infty}^{\infty} x_n e^{in\phi} = 0, & |\phi| < \theta \end{cases} \tag{39}$$

where the expansion coefficients f_n of the right-hand side are supposed to be known and are decreasing as $O(|n|^{-1+\alpha})$, $\alpha > 0$ for great $|n|$. Following [16], an exact analytical solution to this equation can be conveniently written as

$$x_m = \sum_{n=-\infty}^{\infty} f_n T_{mn}(\theta), \qquad m = 0, \pm1, \pm2, \cdots \tag{40}$$

$$T_{mn}(\theta) = \frac{(-1)^{m+n}}{2(m-n)}\left[P_m(-u)P_{n-1}(-u) - P_{m-1}(-u)P_n(-u)\right] \qquad m \ne n,\ u = \cos\theta \tag{41}$$

$$T_{00}(\theta) = -\ln\frac{1-\cos\theta}{2}$$

$$T_{mm}(\theta) = \frac{1}{2|m|}\left\{1 + \sum_{s=1}^{|m|} t_s(-u)P_{s-1}(-u)\right\} \qquad m \ne 0. \tag{42}$$

Here $t_0(-u) = 1$, $t_1(-u) = u$, $t_{s\ge2}(-u) = P_s(-u) + 2uP_{s-1}(-u) + P_{s-2}(-u)$, and P_n are the Legendre polynomials.

2) For a series equation given as

$$\sum_{n=-\infty}^{\infty} x_n e^{in\phi} = \begin{cases} \sum_{n=-\infty}^{\infty} f_n e^{in\phi}, & \theta < |\phi| \le \pi \\ 0, & |\phi| < \theta \end{cases}$$

we apply the inverse Fourier transformation; that is, multiply both sides by $e^{-im\phi}$ and integrate from 0 to 2π. The result is

$$x_m = \sum_{n=-\infty}^{\infty} f_n S_{mn}(\theta), \qquad m = 0, \pm1, \pm2, \cdots \tag{44}$$

$$S_{mn}(\theta) = -\frac{\sin\theta(m-n)}{\pi(m-n)}, \qquad m \ne n,\ S_{mm}(\theta) = 1 - \frac{\theta}{\pi}. \tag{45}$$

Note that both (40) and (44) are the number sequences of the class l_2, i.e., $\sum_{n=-\infty}^{\infty}|x_n|^2 < \infty$.

ACKNOWLEDGMENT

The authors would like to thank A. Matsushima, Department of Electrical and Computer Engineering, Kumamoto University, Japan, for many valuable discussions and V. V. Yachin, Institute of Radio Astronomy, National Academy of Sciences, Ukraine, for providing the comparison data for Fig. 8. They would also like to thank one of the reviewers for helpful advice.

REFERENCES

[1] H. Lamb, "On the reflection and transmission of electric waves by metallic grating," *Proc. London Math. Soc.* vol. 29, no. 1, pp. 523–545, 1898.

[2] Z. S. Agranovich, V. A. Marenko, and V. P. Shestopalov, "Diffraction of a plane electromagnetic wave from plane metallic lattices," *Soviet Phys. Tech. Phys.*, vol. 7, pp. 277–286, 1962 (Engl. transl.).

[3] T. Uchida, T. Noda, and T. Matsunaga, "Spectral domain analysis of electromagnetic wave scattering by an infinite plane metallic grating," *IEEE Trans. Antennas Propagat.,* vol. AP-35, pp. 46–52, Jan. 1987.

[4] A. Matsushima and T. Itakura, "Singular integral equation approach to plane wave diffraction by an infinite strip grating at oblique incidence," *J. Electromagn. Waves Applicat.*, vol. 4, no. 6, pp. 505–519, 1990.

[5] G. Bouchittè and R. Petit, "On the concept of a perfectly conducting material and a perfectly conducting and infinitely thin screen," *Radio Sci.,* vol. 24, no. 1, pp. 13–26, 1989.

[6] A. D. Rawlins, "Diffraction by acoustically penetrable or electromagnetically dielectric half plane," *Int. J. Eng. Sci.*, vol. 15, pp. 569–598, 1977.

[7] E. Bleszynski, M. Bleszynski, and T. Jaroszewicz, "Surface-integral equations for electromagnetic scattering from impenetrable and penetrable sheets," *IEEE Antennas Propagat. Mag.,* vol. 36, no. 6, pp. 14–25, Dec. 1993.

[8] T. B. A. Senior and J. Volakis, *Approximate Boundary Conditions in Electromagnetics.* London, U.K.: IEE Press, 1995.

[9] I. V. Vovk, "Diffraction of sound on a grating of strips having finite transparency," *Soviet Phys. Acoust.*, vol. 25, no. 2, pp. 378–381, 1980 (Engl. transl.).

[10] R. C. Hall and R. Mittra, "Scattering from a periodic array of resistive strips," *IEEE Trans. Antennas Propagat.,* vol. AP-33, pp. 1009–1011, Sept. 1985.

[11] ———, "Analysis of multilayered periodic structures using generalized scattering matrix theory," *IEEE Trans. Antennas Propagat.,* vol. 36, pp. 511–517, Apr. 1988.

[12] R. Petit and G. Tayeb, "Theoretical and numerical study of gratings consisting of periodic arrays of thin and lossy strips," *J. Opt. Soc. Amer.*, vol. 7, pt. A, no. 9, pp. 1686–1692, 1990.

[13] J. L. Volakis, Y. C. Lin, and H. Anastassiu, "TE characterization of resistive strip gratings on a dielectric slab using a single edge-mode expansion," *IEEE Trans. Antennas Propagat.,* vol. 42, pp. 205–213, Feb. 1994.

[14] A. I. Nosich, Y. Okuno, and T. Shiraishi, "Scattering and absorption of E- and H-polarized plane waves by a circularly curved resistive strip," *Radio Sci.*, vol. 31, no. 6, pp. 1733–1742, 1996.

[15] A. N. Nosich, V. B. Yurchenko, and A. Altintas, "Numerically exact analysis of a two-dimensional variable-resistivity reflector fed by a complex-point source," *IEEE Antennas Propagat.*, vol. 45, pp. 1592–1601, Nov. 1997.

[16] R. W. Ziolkowski, "N-series problems and the coupling of the electromagnetic waves to apertures: Riemann–Hilbert approach," *SIAM J. Appl. Math.*, vol. 16, pp. 358–378, 1985.

[17] A. I. Nosich, "Green's function—Dual series approach in wave scattering from combined resonant scatterers," in *Analytical and Numerical Methods in Electromagnetic Wave Theory*, M. Hashimoto, M. Idemen, and O. A. Tretyakov, Eds. Tokyo, Japan: Science House, 1993, ch. 9, pp. 419–469.

[18] R. Orta, P. Savi, and R. Tascone, "The effect of finite conductivity on frequency selective surface behavior," *Electromagn.*, vol. 10, no. 2, pp. 213–227, 1990.

[19] A. D. Rawlins, E. Meister, and F.-O. Speck, "Diffraction by an acoustically transmissive or an electromagnetically dielectric half-plane," *Math. Methods Appl. Sci.*, vol. 14, no. 2, pp. 387–402, 1991.

[20] N. A. Khizhnyak, N. V. Ryazantseva, and V. V. Yachin, "The scattering of electromagnetic waves by a periodic magneto-dielectric layer," *J. Electromagn. Waves Applicat.*, vol. 10, no. 5, pp. 731–739, 1996.

[21] A. Matsushima, T. L. Zinenko, H. Minami, and Y. Okuno, "The integral equation analysis of plane wave scattering from multilayered resistive strip gratings," *J. Electromagn. Waves Applicat.*, vol. 12, pp. 1449–1469, 1998.

Tatiana L. Zinenko was born in Kommunarsk, Ukraine. She received the M.S. degree from the Radio Physics Department, Kharkov State University, Ukraine, in 1982. She is currently working toward the Ph.D. degree at the Ministry of Education of Japan, Monbusho, Japan.

She joined the Institute of Radiophysics and Electronics of the Ukrainian Academy of Science, Kharkov, as a Junior Scientist. From 1996 to 1997 she was with the Department of Computer and Electrical Engineering, Kumamoto University, Japan, as a Research Student on a scholarship from the Ministry of Education of Japan. Her research interests are in integral equation methods and electromagnetic wave scattering from imperfect scatterers and periodic gratings.

Ms. Zinenko is a student member of the Institute of Electronics, Information, and Communication Engineers (IEICE) of Japan.

Alexander I. Nosich (M'94–SM'95) was born in 1953 in Kharkov, Ukraine. He received the M.S., Ph.D., and D.Sc. degrees in radio physics from the Radio Physics Department, Kharkov State University, Ukraine, in 1975, 1979, and 1990, respectively.

Since 1978, he has been on the Research Staff of the Institute of Radiophysics and Electronics (IRE) of the Ukrainian Academy of Sciences, Kharkov. From 1992 to 1997, he held Research Fellowships and Visiting Professorships in Bilkent University, Ankara, Turkey, and Kumamoto University, Gifu University, and Chuo University, all in Tokyo, Japan, University of Rennes 1, France, and Torino Polytechnical University, Italy. Currently, he is with IRE, Kharkov, as a Leading Scientist in the Department of Computational Electromagnetics. Since 1995, he has been on the editorial board of the *International Journal of Microwave and Optical Technology Letters*. His research interests include analytical regularization techniques, with applications to the free-space and open-waveguide scattering, complex mode behavior, radar cross-section, and antenna modeling.

Yoichi Okuno (SM'98) was born in Tokyo, Japan, in 1948. He received the B.E., M.E., and D.E. degrees from Kyushu University, Fukuoka, Japan, in 1973, 1975, and 1978, respectively.

Since 1979, he has been with the Department of Electrical and Computer Engineering, Kumamoto University, Kumamoto, Japan, where he is now a Professor. His research interests include computational methods for electromagnetic boundary-value problems.

Dr. Okuno is a member of the Institute of Electrical Engineers (IEE) of Japan and of the Institute of Electronics, Information, and Communication Engineers (IEICE) of Japan.